Efficient plant male fertility depends on vegetative nuclear movement mediated by two families of plant outer nuclear membrane proteins

Xiao Zhou and Iris Meier[1]

Department of Molecular Genetics, The Ohio State University, Columbus, OH 43210

Edited by Ueli Grossniklaus, Institute of Plant Biology and Zürich-Basel Plant Science Center, University of Zurich, Zurich, Switzerland and accepted by the Editorial Board July 8, 2014 (received for review December 16, 2013)

Increasing evidence suggests that nuclear migration is important for eukaryotic development. Although nuclear migration is conserved in plants, its importance for plant development has not yet been established. The most extraordinary plant nuclear migration events involve plant fertilization, which is starkly different from that of animals. Instead of evolving self-propelled sperm cells (SCs), plants use pollen tubes to deliver SCs, in which the pollen vegetative nucleus (VN) and the SCs migrate as a unit toward the ovules, a fundamental but barely understood process. Here, we report that WPP domain-interacting proteins (WIPs) and their binding partners the WPP domain-interacting tail-anchored proteins (WITs) are essential for pollen nuclear migration. Loss-of-function mutations in *WIT* and/or *WIP* gene families resulted in impaired VN movement, inefficient SC delivery, and defects in pollen tube reception. WIPs are Klarsicht/ANC-1/Syne-1 Homology (KASH) analogs in plants. KASH proteins are key players in animal nuclear migration. Thus, this study not only reveals an important nuclear migration mechanism in plant fertilization but also, suggests that similar nuclear migration machinery is conserved between plants and animals.

nuclear envelope | *Arabidopsis* | male gametophyte | LINC complex

Nuclear migration is essential for cell differentiation, polarization, and migration, which influence organism development (1–3). Examples range from *Caenorhabditis elegans* P-cell development to mammalian neural development (1–3). The key players in opisthokont nuclear migration are the inner nuclear membrane Sad1/UNC-84 (SUN) proteins and outer nuclear membrane Klarsicht/ANC-1/Syne-1 Homology (KASH) proteins. SUN and KASH proteins form the linkers of the nucleoskeleton and the cytoskeleton complexes at the nuclear envelope (NE) and transfer cytoplasmic forces to the nucleus (1–3). In plants, nuclear migration is associated with a number of developmental events and environmental responses, including fertilization, root and leaf hair formation, and plant–microbe interactions (4, 5). So far, little is known about the mechanism of plant nuclear migration. Although SUN proteins are conserved in plants (6, 7), absence of animal KASH homologs in plants suggests that plants may have evolved different molecular solutions to achieve nuclear migration. Recently, WPP domain-interacting proteins (WIPs) were identified as KASH proteins in plants (8), and their outer nuclear membrane binding partners WPP domain-interacting tail anchored proteins (WITs) were shown to interact with myosin XI-I (9). The WIT–myosin XI-I complexes regulate nuclear movement in root and mesophyll cells, but no developmental events have been linked to these nuclear movements (9).

Essential for plant fertility, pollen tube growth harbors the most dramatic nuclear movement in plants. Unlike animals, which have sperm cells (SCs) that travel through self-propelled flagellum, flowering plants use pollen tubes to deliver SCs to ovules (10–13). In *Arabidopsis*, pollen tube growth is guided by chemical cues in carpel tissues and attracted by small peptides secreted by synergid cells in the vicinity of ovules (14–18). Pollen tube reception is completed by pollen tube burst, SC release, and degeneration of synergid cells (12). If this process fails, a second pollen tube can be attracted to the same ovule for a second attempt, resulting in polytubey (19). The SCs [or their progenitor the generative cell (GC)] are enclosed by an endocytic membrane tethered to the pollen vegetative nucleus (VN) (20). During pollen tube elongation, the VN and the SCs/GC are usually closely associated and move as a male germ unit (MGU) (13, 21). For decades, the movement of the MGU has been analyzed using cytoskeleton-depolymerizing reagents or heterogeneous antimyosin antibodies (22–27). However, no genes have been implicated in MGU movement, and the function of the joint migration of VN and GC/SC remains hypothetical.

Here, we have identified the *Arabidopsis* WIT and WIP protein families as key players in VN movement. WIP1 and WIT1 are localized at the vegetative nuclear envelope (VNE). Loss of either WIT or WIP family proteins impaired VN movement, resulting in defective pollen tube reception and inefficient SC-to-ovule migration. This study has not only identified a molecular mechanism regulating the VN movement but also, revealed an important function of the VN in plant fertilization.

Results

***WIT* and *WIP* Are Required for Full Seed Set.** In *Arabidopsis*, WIT and WIP are two families of NE-associated proteins that synergistically anchor Ran GTPase-activating protein 1 (RanGAP1) to the NE (28, 29). Reduction in seeds per silique was observed

Significance

Double fertilization of the female gametophyte is vital for angiosperm reproduction and requires delivery of sperm cells through a pollen tube. The sperm cells and pollen vegetative nucleus together are called the male germ unit. The pollen tube grows a long distance from the stigma to the ovary, and the mode of male germ unit movement and sperm cell delivery is largely unknown. This study reveals that WPP domain-interacting protein, a plant analog of animal proteins known to control nuclear movement, and WPP domain-interacting tail-anchored protein are responsible for movement of the vegetative nucleus within pollen tubes and contribute to sperm cell-to-ovule migration. This finding marks a leap forward in our understanding of double fertilization and the mechanism of nuclear movement in plants as a whole.

Author contributions: X.Z. and I.M. designed research; X.Z. performed research; X.Z. and I.M. analyzed data; and X.Z. and I.M. wrote the paper.

The authors declare no conflict of interest.

This article is a PNAS Direct Submission. U.G. is a guest editor invited by the Editorial Board.

[1]To whom correspondence should be addressed. Email: meier.56@osu.edu.

This article contains supporting information online at www.pnas.org/lookup/suppl/doi:10.1073/pnas.1323104111/-/DCSupplemental.

in *wit1-1 wit2-1* double null (*wit12*; ~50% loss) (Fig. 1*A*) and *wip1-1 wip2-1 wip3-1* triple null (*wip123*; ~33% loss) (Fig. 1*A*). In contrast, the number of seeds per silique of *wit1-1*, *wit2-1*, *wip1-1 wip2-1*, *wip2-1 wip3-1*, and *wip1-1 wip3-1* mutants was only slightly reduced compared with WT (Fig. 1*A*). Ovaries of *wit12* and *wip123* contain, on average, four ovules fewer than WT (Fig. 1*B*), which is unlikely to cause the significantly reduced seed production. The quintuple null mutant *wip1-1 wip2-1 wip3-1 wit1-1 wit2-1* (*wifi*) has the most severe seed loss phenotype, suggesting that *WIT* and *WIP* synergistically affect seed production (Fig. 1*A*). As shown in Fig. 1*A*, *WIT1* promoter-driven *GFP-WIT1* (*WIT1pro::GFP-WIT1*) rescued (Fig. 1*A*, lines 1 and 3) or partially rescued (Fig. 1*A*, line 2) *wit12*, and *WIP1* promoter-driven *GFP-WIP1* (*WIP1pro::GFP-WIP1*) rescued (Fig. 1*A*, lines 2 and 3) or partially rescued (Fig. 1*A*, line 1) *wip123*. These data indicate that this phenotype is linked to the *wit* or *wip* mutations.

Loss of *WIT* or *WIP* Leads to Male Fertility Defects. To analyze the parental origin of the seed loss, we performed reciprocal crosses between WT and *wit12*. As shown in Fig. 1*C*, when pollinated with WT pollen, both *wit12* and WT developed similar numbers of seeds per silique. In contrast, when pollinated with *wit12* pollen, both *wit12* and WT developed only roughly one-half the amount of seeds per silique compared with hand-pollinated WT with WT pollen. Reciprocal crosses were also performed between WT and *wip123* and between WT and *wifi*. Similar results were obtained (Fig. 1*C*).

We then examined the expression and localization pattern of WIT1 and WIP1 in the pollen of *WIT1pro::GFP-WIT1*–rescued *wit12* lines or the *WIP1pro::GFP-WIP1*–rescued *wip123* lines. Both GFP-WIT1 and GFP-WIP1 signals were strongly associated with the VNE (Fig. 2*A* and Fig. S1 *A* and *B*). In addition,

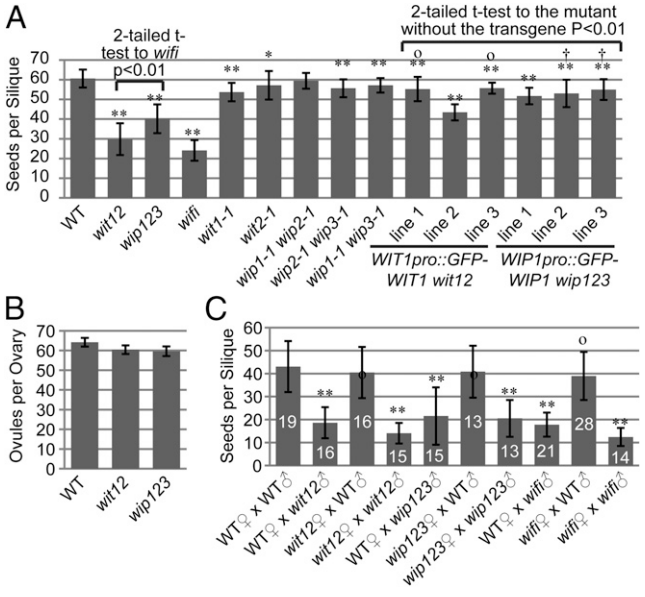

Fig. 1. Reduction in seed production based on loss of *WIT* and/or *WIP*. (*A*) Number of seeds per silique compared between different mutants and lines. *0.01 < *P* < 0.05 compared with WT. **$P < 0.01$ compared with WT. $^{o}P > 0.05$ compared with *wit2-1*. $^{\dagger}P > 0.05$ compared with *wip2-1 wip3-1*. $n = 40$ for all samples. (*B*) Number of ovules per ovary of WT, *wit12*, and *wip123* ($n = 10$). (*C*) Number of seeds per silique after reciprocal crosses between WT and *wit12*, between WT and *wip123*, or between WT and *wifi*. **$P < 0.01$ compared with WT♀ × WT♂. $^{o}P > 0.05$ compared with WT♀ × WT♂. The *n* for each dataset was indicated on the graph. In *A*–*C*, error bars in all histograms represent SD, and two-tailed *t* test was used for statistical analysis.

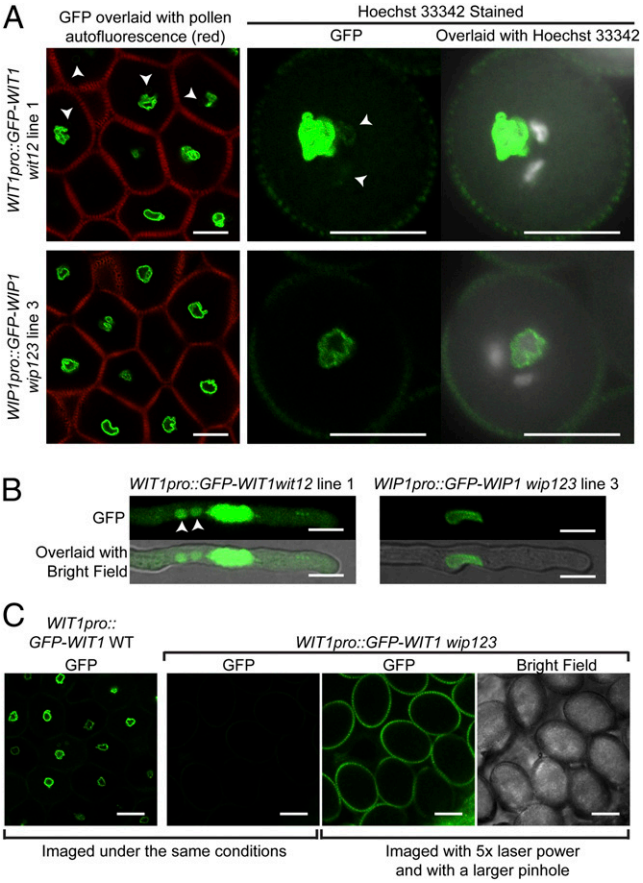

Fig. 2. WIT1 and WIP1 subcellular localization in pollen grains and pollen tubes. (*A*) The localization of WIT1 and WIP1 in pollen grains was examined using *WIT1pro::GFP-WIT1 wit12* line 1 and *WIP1pro::GFP-WIP1 wip123* line 3, respectively. GFP signal was imaged by confocal microscopy, and the Hoechst 33342 signal was imaged by fluorescence microscopy. The autofluorescence from pollen walls was collected through the RFP channel and merged with the GFP signal in the images in *Left*. GFP-WIT1 and GFP-WIP1 were both localized at the VNE. In addition, GFP-WIT1 also weakly labeled the SC NE (arrowheads). (*B*) *WIT1pro::GFP-WIT1 wit12* line 1 and *WIP1pro::GFP-WIP1 wip123* line 3 pollen tubes after 5 h of pollen germination. GFP-WIT1 was strongly localized at the VNE, and it was also visible in the SCs, probably the SC NE (arrowheads), whereas GFP-WIP1 was only detectable at the VNE. Imaging conditions were tuned to view the signal in the SCs, and therefore, the GFP signals at the VNE are saturated and appear nuclear. (*C*) Compared with its protein level in WT, GFP-WIT1 was barely detectable in *wip123* pollen grains. (Scale bars: 10 μm.)

GFP-WIT1 weakly labeled the SC NE in some pollen grains (Fig. 2*A* and Fig. S1*A*). After 5 h of in vitro growth of pollen tubes, GFP-WIT1 and GFP-WIP1 were visible at the VNE, and WIT1 was also weakly visible in SCs, probably the SC NE (Fig. 2*B*). WT plants carrying the *WIT1pro::GFP-WIT1* or *WIP1pro::GFP-WIP1* transgene revealed similar results (Fig. S1*B*). It has been reported that the WIT1 protein level is significantly reduced in *wip123* vegetative tissues, likely because the protein is destabilized/degraded in the absence of the WIP–WIT complex (29). The GFP-WIT1 signal is also barely detectable in *wip123* pollen (three lines were examined, and a representative image is shown in Fig. 2*C*), which agrees with the previous report and suggests that the reduced fertility phenotype of *wip123* is, to a large extent, caused by the loss of WIT proteins.

To assess the influence of the *wit* or *wip* mutation on male fertility, pollen competition assays were performed between WT pollen and (*i*) *wit12* pollen, (*ii*) *WIT1pro::GFP-WIT1 wit12* line 1

pollen, (*iii*) *wip123* pollen, or (*iv*) *WIP1pro::GFP-WIP1 wip123* line 3 pollen. As shown in pollen competition experiments (Fig. S1*C*), *wit12* and *wip123* have a much reduced transmission efficiency (3.9% and 13.3%, respectively), whereas *WIT1pro::GFP-WIT1* and *WIP1:GFP-WIP1* rescued the transmission efficiency to the WT level (50%).

These data indicate that *WIT* and *WIP* are essential for male fertility. This defect is clearly different from the female gametophyte lethality caused by mutating RanGAP1 and RanGAP2 (30), suggesting that maintaining pollen fertility is a function of WIT and WIP independent of their reported role as RanGAP NE anchors.

***WIT* and *WIP* Are Required for Proper Nuclear Movement in Pollen Tubes.** We then examined *wit12*, *wip123*, and *wifi* pollen in detail. The morphology of mutant anthers and pollen grains is normal, and no significant amount of dead pollen was observed using Alexander staining (Fig. S1*D*). The three nuclei—one VN and two SC nuclei (SN)—are also normal (Fig. S1*E*). Because WIPs are plant KASH proteins and WITs are involved in root and leaf nuclear movement (8, 9), we monitored nuclear movement in pollen tubes germinated in vitro. mCherry tagged with a nuclear localization signal and driven by the *ubiquitin 10* promoter was used as a VN marker (*VN-RFP*) (31). *MGH3/HRT10*, a male gamete-specific histone H3 gene fused with GFP and driven by the *MGH3* promoter, was used as an SN marker (*SN-GFP*) (32).

As shown in Fig. 3*A* and Movie S1, during WT pollen germination, typically, the VN entered the pollen tube first when the pollen tube reached a certain length (we define the tube length when the first nucleus permanently enters the pollen tube as the entrance length, which is quantified in Fig. S2*A*). As observed in many plant species (13), the VN precede the SCs as they move along the growing pollen tube. The VN also remained at a certain distance from the growing tip followed by the SN. In contrast to WT, as shown in Fig. 3*B* and Movie S2, when *wit12* pollen tubes had reached their much greater entrance length (Fig. S2*A*), the two SN typically entered the pollen tube first (Fig. S2*B*), and the two SN then led the VN in the growing pollen tubes (Fig. 3*B* and Movie S2). Measuring the leading SN-to-tip distance every 1 min for 60 min after the two SN had entered the pollen tube, a mean value of 56.2 μm (SD = 31.2 μm, 10 pollen tubes were measured) was obtained, much larger than that of WT (Fig. S2*C*).

We then examined the nuclear position in in vitro-germinated pollen tubes at 5 h, a time point when in vivo pollen tubes would start entering the micropyle (33). In nearly all *wit12* pollen tubes, the two SN were still ahead of the VN, significantly different from WT (Fig. 3*C*). A similar phenotype was also observed in Hoechst 33342-stained *wip123* and *wifi* pollen tubes after 5 h in vitro germination (Fig. 3*C*). Consistently, the transgenic mutant lines with seed loss phenotype that was rescued showed normal nuclear positioning after 5 h of in vitro germination (Fig. 3*C*). Recently, myosin XI-I was reported to be recruited to the NE by WIT1 and WIT2 and regulate nuclear movement in roots and mesophyll cells (9). However, *kaku1-4*, a reported *myosin xi-i* null mutant (9), exhibits normal seeds per silique and normal nuclear order after 5 h of in vitro pollen germination (Fig. S2 *D* and *E*), consistent with the report that no nuclear migration defects were observed in *kaku1-4* (9).

Investigating semi-in vivo germinated pollen tubes 8 h after germination—the time when double fertilization starts in vivo (33)—we discovered that the nuclear order was still reversed in *wit12* pollen tubes (Fig. S3*A*). More interestingly, unlike the closely associated VN and SN in WT, isolated VN (Fig. S3*A*, dotted line) and solely migrating SN (Fig. S3*A*, arrowheads) were observed in *wit12* pollen tubes (Fig. S3*A*). We examined this phenotype in detail 16 h after semi-in vivo pollen germination. *RanGAP1pro::RanGAP1-GFP* was used as an additional marker

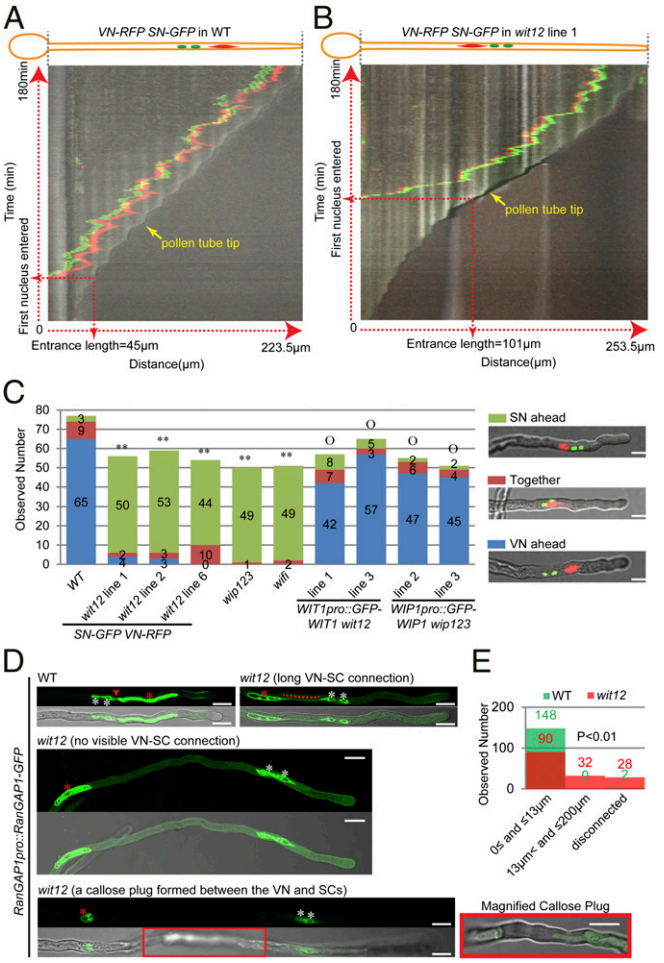

Fig. 3. Nuclear movement in pollen tubes is affected in *wit12*, *wip123*, and *wifi*. (*A*) Kymograph of nuclear movement in a *VN-RFP SN-GFP* WT pollen tube. Vertical axis represents time (total = 180 min), and horizontal axis represents the distance along the pollen tube (total pollen tube length = 223.5 μm). (*B*) Kymograph of nuclear movement in a *VN-RFP SN-GFP wit12* pollen tube. Vertical axis represents time (total = 180 min), and horizontal axis represents the distance along the pollen tube (total pollen tube length = 253.5 μm). (*C*) Nuclear order in pollen tubes after 5 h of germination. An example of each category is shown in *Right*. For *wip123*, *wifi*, and *WIP1pro::GFP-WIP1 wip123* pollen tubes, Hoechst 33342 was used to stain DNA, and confocal microscopy was used for the others. Two-tailed Fisher exact test was used for statistical analysis, and numbers for each category are indicated on the graph. $^{**}P < 0.01$ compared WT. $^{O}P > 0.05$ compared with WT. (Scale bars: 10 μm.) (*D*) Position of the VN (red asterisks) relative to the SCs (white asterisks) after 16 h of semi-in vivo germination. In WT pollen tubes, the VN was closely associated with the SCs, and the connection (red arrowhead) was visible. However, in the *wit12* pollen tubes, the connections were longer (red dotted line), undetectable, or interrupted by a callose plug (red box that is magnified at a focal plane clearly showing the plug). For each example, GFP signal is shown in the upper part, and the overlay with a bright-field image is shown in the lower part. The two examples in *Middle* and *Bottom* are maximum projections of *z*-stack images. *Bottom* was assembled from three continuous images by image stitching. (Scale bars: 10 μm.) (*E*) Quantification of the VN–SC distance after 16 h of semi-in vivo pollen germination. The shortest distance between the VNE and SC NE was measured. For either WT or *wit12*, one *VN-RFP SN-GFP* line and two *RanGAP1pro::RanGAP1-GFP* lines were used. Fifty pollen tubes were measured for each line. The VN, which were blocked by a callose plug or undetectable in over 300-μm pollen tubes, were considered disconnected. The numbers are indicated (green, WT; red, *wit12*). $P < 0.01$ represents the statistically significant difference between WT and *wit12* ($P < 0.01$, $n = 150$, two-tailed Fisher exact test).

to visualize the physical connection between the VN and the SCs, because RanGAP1 labels both the VNE and the SC cytoplasm. As shown in Fig. 3*D*, a close VN–SC connection was visible in WT pollen tubes. The VN–SN distance (the closest distance between the VNE and the SC NE) was quantified (Fig. 3*E*), and 99% of WT pollen tubes had a VN–SN distance ≤13 μm. In contrast, for *wit12* pollen tubes, only 60% fell in this range, and 21% had a much longer VN–SN distance (>13 but ≤200 μm), and in 19% of pollen tubes, the VN was either blocked by a callose plug or undetectable (disconnected) (Fig. 3 *D* and *E*). However, the VN movement defect of *wit12* does not impair pollen germination or pollen tube length (details are in Fig. S3 *B–D*).

Loss of *WIT* or *WIP* Impaired the Pollen Tube Reception and SC-to-Ovule Migration. To determine the cause of male fertility defects in *wit12*, WT pistils expressing *NLS-2xRFP* (nuclear localization signal fused to double red fluorescent protein) under the *Egg Cell 1 promoter* (*EC1pro::NLS-2xRFP*) were pollinated with *wit12* pollen expressing *GFP* under the *Lat52 promoter* (*Lat52-pro::GFP*). The ovules were examined after 24 h. As shown in Fig. 4 *A* and *B*, only 45% of pollen tubes burst, whereas 21% stalled at the micropyle, and 34% overgrew into the ovules. Ovules that had attracted two pollen tubes were also observed occasionally (Fig. 4*C*). In contrast, ∼99% of *Lat52pro::GFP* WT pollen tubes burst.

We then dissected and examined *wit12* ovaries ∼72 h after flower opening. Two types of ovules were found in *wit12* ovaries—large fertilized ovules with visible developing embryos and small unfertilized ovules with central cell nuclei that were clearly visible (Fig. S4 *A* and *B*). A similar phenotype was also observed in the ovaries of *wip123* and *wifi* (Fig. S4*A*). The number of large fertilized ovules per ovary of WT and *wit12* was slightly lower than their average seeds per silique (compare Fig. 1*A* with Fig. S4*C*), suggesting that a small fraction of the unfertilized ovules scored would still become fertilized. Aniline blue staining of the ovules of *wit12* or imaging of the ovules of the *Lat52pro::GFP wit12* at this stage revealed both overgrowth and polytubey abnormalities (Fig. S5 *A* and *B*), similar to the pollen tube defects of *wit12* 24 h after pollination (Fig. 4*A*). These two abnormalities are more common in unfertilized ovules— among 302 examined ovules, 64 (21%) ovules displayed polytubey phenotype, and 187 (62%) ovules exhibited overgrown pollen tubes (Table 1). Similar abnormalities were also observed in the ovaries of *wip123* (Table 1 and Fig. S5*A*).

To determine the localization of SN and VN in the unfertilized ovules, confocal microscopy was used to image the small unfertilized ovules of *VN-RFP SN-GFP wit12*. As shown in Fig. 4*D* and Fig. S5*C*, the two SN were arrested in the vicinity of the ovules (39%), at the micropyle (44%), or inside the ovules (18%), reflecting a severe SC-to-ovule migration defect. In none of the analyzed ovules was a VN visible. Because the semi-in vivo assay shows that the VN can be disconnected from the SCs during migration (Fig. 3 *D* and *E* and Fig. S3*A*), we hypothesize that the VN might never reach the vicinity of these ovules. To assess this possibility under more native conditions, pollen grains were germinated 24 h on pistils with ovaries that were cut to a length of ∼600 μm, and the pollen tubes that grew through the pistils were examined. Pollen tubes with both the VN and the SCs detectable within 250 μm from the tips were considered as intact MGU emerged; otherwise, they were considered as no intact MGU emerged. As shown in Fig. S5*D*, 40% of *wit12* pollen tubes had no intact MGU emerged, which supports our hypothesis. Together, these data suggest that *wit12* exhibits severe impairment in pollen tube reception and SC-to-ovule migration.

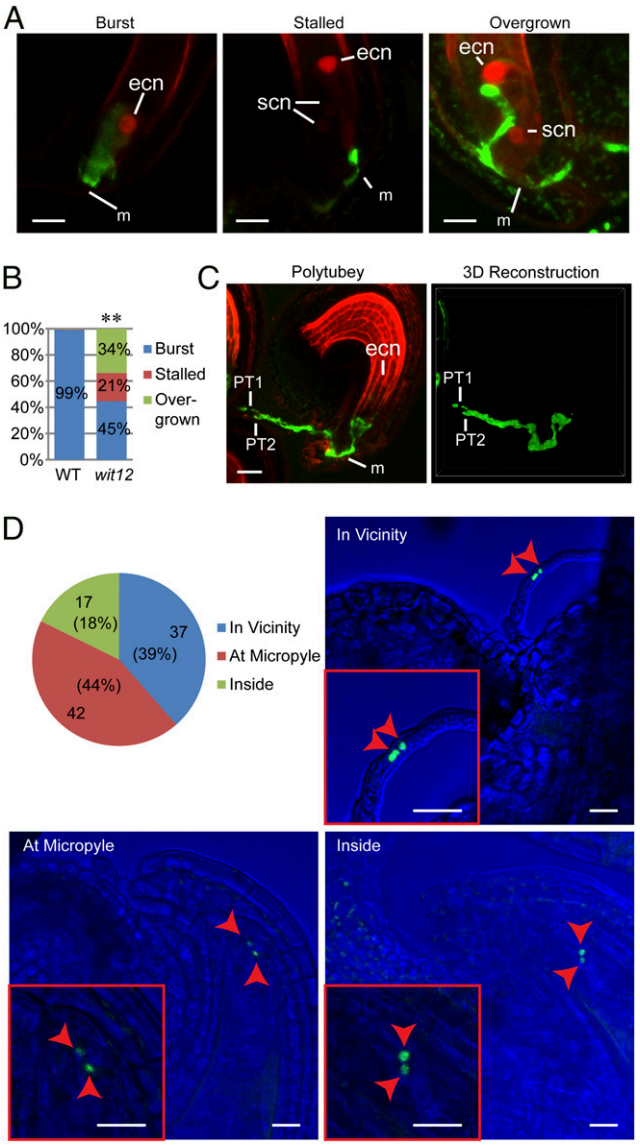

Fig. 4. Defects of pollen tube reception and SC-to-ovule migration in *wit12*. (*A*) *EC1pro::NLS-2xRFP* WT pistils were pollinated with *Lat52pro::GFP* WT pollen or *Lat52pro::GFP wit12* pollen. The pistils were dissected and imaged 24 h later. The *wit12* pollen tubes showed three types of fate: burst (WT like), stalled [stopped at the micropyle (m) but did not burst], and overgrown inside ovules. The stalled and overgrown images are maximum projections of *z*-stack images, which were processed with a 5-pixel median filter to reduce background noise. NLS-2xRFP strongly labeled the egg cell nuclei (ecn) and also weakly labeled the synergid cell nuclei (scn). (Scale bars: 10 μm.) (*B*) Quantification of the three types of *wit12* pollen tube fate observed in *A*. The percentage of each category is indicated on the graph. For WT, $n = 270$, and for *wit12*, $n = 170$. $^{**}P < 0.01$ compared with WT (two-tailed Fisher exact test). (*C*) Two *Lat52pro::GFP wit12* pollen tubes were attracted to one *EC1pro::NLS-2xRFP* WT ovule 24 h after pollination. *Left* is a maximum projection of a *z*-stack image processed with 5-pixel median filter to reduce background noise. *Right* is a 3D reconstruction of its GFP channel using α-blending. PT1, pollen tube 1; PT2, pollen tube 2. (Scale bar: 20 μm.) (*D*) The SC fate in the pollen tubes that targeted small unfertilized ovules of self-pollinated *VN-RFP SN-GFP wit12* was examined 72 h after flower opening. The SN were found in the vicinity of an ovule, at the micropyle of an ovule, or inside an ovule. These three categories are quantified in the pie chart, and representative examples are shown. The bright field was tuned to dark blue for better exhibition of the SN. Arrowheads indicate the SN. (Scale bars: 20 μm.)

Table 1. Quantification of pollen tube reception defects of *wit12* and *wip123*

	WT		*wit12*		*wip123*	
Pollen tube morphology	Big fertilized ovules	Small unfertilized ovules	Big fertilized ovules	Small unfertilized ovules	Big fertilized ovules	Small unfertilized ovules
With pollen tubes; not overgrown	265	2	138	77	118	39
With overgrown pollen tubes	0	1	3	187	12	48
Without pollen tubes	0	4	0	38	0	10
Total	265	7	141	302	130	97
Among total: ovules with polytubey	10	1	14	64	16	19

Discussion

The MGU has been observed in many plant species (13), and our analysis of in vitro-geminated *Arabidopsis* pollen shows that the VN and SCs do form a linked unit that moves together along growing pollen tubes (Movie S1). Even in the *wit12* mutant, with a VN that seemingly loses its driving force, the VN was still connected to and moved in conjunction with the SCs (Movie S2), reflecting a functional linkage between the VN and SCs. During WT pollen tube growth, the VN entered the pollen tube first and led the movement of SCs with occasionally backward movement when the MGU was extremely close to the tip of the growing tube (Fig. 3*A* and Movie S1). SCs coordinated with this movement exhibited transient position shifts with the VN (Fig. 3*A* and Movie S1). Although the mobility of the VN is impaired in *wit12* and the entrance length is longer than that of WT, the distance-keeping ability of the MGU is not totally lost: the SCs led the movement of the MGU and made back-and-forth adjustment according to the distance to the growing tube apex (Fig. 3*B* and Movie S2). Even when the VN was disconnected from the SCs, the SCs still moved forward (Fig. 3*D* and Fig. S3*A*). These observations indicate that there are (*i*) a main driving force transferred through WITs that moves the VN, (*ii*) a secondary driving force facilitating the movement of the SCs, and (*iii*) a signaling mechanism between the VN–SC and the growing tip regulating the two driving forces to maintain proper nucleus–tip distance. Because the VN and the two SCs are connected, these two forces coordinate with each other to move the MGU forward. This double-driving force hypothesis is consistent with a reported observation that the SC projection that links the VN exhibited somewhat independent movement to the overall momentum of SCs (34). In addition, the bidirectional movement of the MGU was proposed to be a result of the dynamic balance between acropetal and basipetal forces (35). Although the nuclear order defects and the increased leading nucleus-to-tip distance of *wit12* mimics the nuclear movement in the *Galanthus nivalis* pollen tubes after microtubule depolymerization (24), the question of whether the MGU movement is regulated by the F-actin network or the microtubule network still needs additional investigation, because myosin has also been proposed to move the MGU in pollen tubes of *Lilium longiflorum* and *Nicotiana alata* (26).

The fact that the VN and GC/SCs migrate as a unit has been proposed to be important for efficient SC-to-ovule migration (13, 21, 36). This model is supported by the inefficient migration of SCs in *wit12* with VN movement that is impaired (Figs. 3 and 4*D* and Fig. S5*D*). However, positioning the VN close to the growing pollen tube tip probably plays additional important roles in pollen tube reception, which was implied by the overgrown and stalled pollen tubes (Fig. 4 *A*–*C* and Fig. S5 *A*–*C*). Pollen tube reception involves players from both male and female gametophytes. In *Arabidopsis*, synergid-expressed FERONIA, NORTIA, and LORELEI are essential for pollen tube reception, and their mutants display overgrown pollen tubes (37–41). On the pollen side, ANXUR1 and -2 may be involved in pollen reception (42, 43). Three pollen tube-expressed MYB transcription factors (MYB97, MYB101, and MYB120) were identified as regulating pollen tube gene expression and SC release (44, 45). These findings suggest that, on pollen tube arrival, signaling cascades are triggered in both pollen tubes and synergids. Positioning the VN close to the pollen tube tip might ensure that (*i*) transcripts from the VN required for sensing synergid contact have to be translated at the pollen tube tip and/or (*ii*) synergid feedback signals can only reach a tip-positioned VN for an adequate gene expression response. In support of the latter scenario, in neuroepithelium progenitor cells, the nuclei were shown to oscillate between apical and basal positions to sense the Notch gradient (46).

In summary, WIT and WIP family proteins are localized at the VNE and mediate VN migration during pollen tube growth. Our data support that a mechanism that regulated VN movement is important for SC-to-ovule migration and pollen tube reception. To our knowledge, *WIT*s and *WIP*s are the first genes identified in pollen nuclear migration and can now serve as a base to reveal the full molecular picture of this important process.

Methods

For in vitro pollen germination, pollen grains from the stamens of fully opened flowers were germinated on a pollen germination medium. For semi-in vitro pollen germination, stage 14 *male sterility 1* stigmas were saturated with pollen and incubated on pollen germination medium. For ovules imaged at 72 h after flower opening, a magnifier was used to identify early-stage 13 flower buds (47), which were tagged and collected 72 h later. All procedures are described in *SI Methods*.

ACKNOWLEDGMENTS. We thank Drs. Xianfeng Xu, Qiao Zhao, and Jelena Brkljacic for help in constructing the *wifi* mutant; Ms. Anna Griffis for wording the significance statement; Drs. R. Keith Slotkin and Anna Dobritsa for numerous helpful discussions and donation of the pollen nuclear markers; and Dr. Ravishankar Palnivelu for help with the pollen in vitro germination assay. Financial support was through National Science Foundation Grant NSF-MCB 1243844.

1. Starr DA, Fridolfsson HN (2010) Interactions between nuclei and the cytoskeleton are mediated by SUN-KASH nuclear-envelope bridges. *Annu Rev Cell Dev Biol* 26:421–444.
2. Gundersen GG, Worman HJ (2013) Nuclear positioning. *Cell* 152(6):1376–1389.
3. Rothballer A, Schwartz TU, Kutay U (2013) LINCing complex functions at the nuclear envelope: What the molecular architecture of the LINC complex can reveal about its function. *Nucleus* 4(1):29–36.
4. Takagi S, Islam MS, Iwabuchi K (2011) Dynamic behavior of double-membrane-bounded organelles in plant cells. *International Review of Cell and Molecular Biology*, ed Kwang WJ (Academic, London), Vol 286, pp 181–222.
5. Zhou X, Meier I (2013) How plants LINC the SUN to KASH. *Nucleus* 4(3):206–215.
6. Oda Y, Fukuda H (2011) Dynamics of *Arabidopsis* SUN proteins during mitosis and their involvement in nuclear shaping. *Plant J* 66(4):629–641.
7. Graumann K, Runions J, Evans DE (2010) Characterization of SUN-domain proteins at the higher plant nuclear envelope. *Plant J* 61(1):134–144.
8. Zhou X, Graumann K, Evans DE, Meier I (2012) Novel plant SUN-KASH bridges are involved in RanGAP anchoring and nuclear shape determination. *J Cell Biol* 196(2):203–211.
9. Tamura K, et al. (2013) Myosin XI-i links the nuclear membrane to the cytoskeleton to control nuclear movement and shape in *Arabidopsis*. *Curr Biol* 23(18):1776–1781.
10. Beale KM, Johnson MA (2013) Speed dating, rejection, and finding the perfect mate: Advice from flowering plants. *Curr Opin Plant Biol* 16(5):590–597.

11. Lausser A, Kliwer I, Srilunchang KO, Dresselhaus T (2010) Sporophytic control of pollen tube growth and guidance in maize. *J Exp Bot* 61(3):673–682.
12. Kessler SA, Grossniklaus U (2011) She's the boss: Signaling in pollen tube reception. *Curr Opin Plant Biol* 14(5):622–627.
13. McCue AD, Cresti M, Feijó JA, Slotkin RK (2011) Cytoplasmic connection of sperm cells to the pollen vegetative cell nucleus: Potential roles of the male germ unit revisited. *J Exp Bot* 62(5):1621–1631.
14. Shimizu KK, Okada K (2000) Attractive and repulsive interactions between female and male gametophytes in *Arabidopsis* pollen tube guidance. *Development* 127(20): 4511–4518.
15. Johnson MA, Preuss D (2002) Plotting a course: Multiple signals guide pollen tubes to their targets. *Dev Cell* 2(3):273–281.
16. Jones-Rhoades MW, Borevitz JO, Preuss D (2007) Genome-wide expression profiling of the *Arabidopsis* female gametophyte identifies families of small, secreted proteins. *PLoS Genet* 3(10):1848–1861.
17. Okuda S, et al. (2009) Defensin-like polypeptide LUREs are pollen tube attractants secreted from synergid cells. *Nature* 458(7236):357–361.
18. Takeuchi H, Higashiyama T (2012) A species-specific cluster of defensin-like genes encodes diffusible pollen tube attractants in *Arabidopsis*. *PLoS Biol* 10(12):e1001449.
19. Maruyama D, et al. (2013) Independent control by each female gamete prevents the attraction of multiple pollen tubes. *Dev Cell* 25(3):317–323.
20. Hamamura Y, et al. (2011) Live-cell imaging reveals the dynamics of two sperm cells during double fertilization in Arabidopsis thaliana. *Curr Biol* 21(6):497–502.
21. Dumas C, Knox RB, Gaude T (1985) The spatial association of the sperm cells and vegetative nucleus in the pollen grain of *Brassica*. *Protoplasma* 124(3):168–174.
22. Åström H, Sorri O, Raudaskoski M (1995) Role of microtubules in the movement of the vegetative nucleus and generative cell in tobacco pollen tubes. *Sex Plant Reprod* 8(2): 61–69.
23. Kaul V, Theunis CH, Palser BF, Knox RB, Williams EG (1987) Association of the generative cell and vegetative nucleus in pollen tubes of *Rhododendron*. *Ann Bot* 59(2): 227–235.
24. Heslop-Harrison J, Heslop-Harrison Y, Cresti M, Tiezzi A, Moscatelli A (1988) Cytoskeletal elements, cell shaping and movement in the angiosperm pollen tube. *J Cell Sci* 91(1):49–60.
25. Tirlapur UK, et al. (1995) Confocal imaging and immunogold electron microscopy of changes in distribution of myosin during pollen hydration, germination and pollen tube growth in *Nicotiana tabacum* L. *Eur J Cell Biol* 67(3):209–217.
26. Miller DD, Scordilis SP, Hepler PK (1995) Identification and localization of three classes of myosins in pollen tubes of *Lilium longiflorum* and *Nicotiana alata*. *J Cell Sci* 108(Pt 7):2549–2563.
27. Heslop-Harrison J, Heslop-Harrison Y (1989) Myosin associated with the surfaces of organelles, vegetative nuclei and generative cells in angiosperm pollen grains and tubes. *J Cell Sci* 94(2):319–325.
28. Xu XM, Meulia T, Meier I (2007) Anchorage of plant RanGAP to the nuclear envelope involves novel nuclear-pore-associated proteins. *Curr Biol* 17(13):1157–1163.
29. Zhao Q, Brkljacic J, Meier I (2008) Two distinct interacting classes of nuclear envelope-associated coiled-coil proteins are required for the tissue-specific nuclear envelope targeting of *Arabidopsis* RanGAP. *Plant Cell* 20(6):1639–1651.
30. Rodrigo-Peiris T, Xu XM, Zhao Q, Wang H-J, Meier I (2011) RanGAP is required for post-meiotic mitosis in female gametophyte development in *Arabidopsis thaliana*. *J Exp Bot* 62(8):2705–2714.
31. Schönberger J, Hammes UZ, Dresselhaus T (2012) In vivo visualization of RNA in plants cells using the λN_{22} system and a GATEWAY-compatible vector series for candidate RNAs. *Plant J* 71(1):173–181.
32. Ingouff M, Hamamura Y, Gourgues M, Higashiyama T, Berger F (2007) Distinct dynamics of HISTONE3 variants between the two fertilization products in plants. *Curr Biol* 17(12):1032–1037.
33. Faure JE, Rotman N, Fortuné P, Dumas C (2002) Fertilization in *Arabidopsis thaliana* wild type: Developmental stages and time course. *Plant J* 30(4):481–488.
34. Ge L, et al. (2011) Migration of sperm cells during pollen tube elongation in *Arabidopsis thaliana*: Behavior during transport, maturation and upon dissociation of male germ unit associations. *Planta* 233(2):325–332.
35. Heslop-Harrison J, Heslop-Harrison Y (1989) Actomyosin and movement in the angiosperm pollen tube: An interpretation of some recent results. *Sex Plant Reprod* 2(4): 199–207.
36. Russell SD, Cass DD (1981) Ultrastructure of the sperms of *Plumbago zeylanica* 1. Cytology and association with the vegetative nucleus. *Protoplasma* 107(1-2):85–107.
37. Huck N, Moore JM, Federer M, Grossniklaus U (2003) The *Arabidopsis* mutant *feronia* disrupts the female gametophytic control of pollen tube reception. *Development* 130(10):2149–2159.
38. Escobar-Restrepo JM, et al. (2007) The FERONIA receptor-like kinase mediates male-female interactions during pollen tube reception. *Science* 317(5838):656–660.
39. Kessler SA, et al. (2010) Conserved molecular components for pollen tube reception and fungal invasion. *Science* 330(6006):968–971.
40. Capron A, et al. (2008) Maternal control of male-gamete delivery in *Arabidopsis* involves a putative GPI-anchored protein encoded by the *LORELEI* gene. *Plant Cell* 20(11):3038–3049.
41. Tsukamoto T, Qin Y, Huang Y, Dunatunga D, Palanivelu R (2010) A role for LORELEI, a putative glycosylphosphatidylinositol-anchored protein, in *Arabidopsis thaliana* double fertilization and early seed development. *Plant J* 62(4):571–588.
42. Miyazaki S, et al. (2009) *ANXUR1* and *2*, sister genes to *FERONIA/SIRENE*, are male factors for coordinated fertilization. *Curr Biol* 19(15):1327–1331.
43. Boisson-Dernier A, et al. (2009) Disruption of the pollen-expressed *FERONIA* homologs *ANXUR1* and *ANXUR2* triggers pollen tube discharge. *Development* 136(19): 3279–3288.
44. Leydon AR, et al. (2013) Three MYB transcription factors control pollen tube differentiation required for sperm release. *Curr Biol* 23(13):1209–1214.
45. Liang Y, et al. (2013) MYB97, MYB101 and MYB120 function as male factors that control pollen tube-synergid interaction in *Arabidopsis thaliana* fertilization. *PLoS Genet* 9(11):e1003933.
46. Del Bene F, Wehman AM, Link BA, Baier H (2008) Regulation of neurogenesis by interkinetic nuclear migration through an apical-basal notch gradient. *Cell* 134(6): 1055–1065.
47. Smyth DR, Bowman JL, Meyerowitz EM (1990) Early flower development in Arabidopsis. *Plant Cell* 2(8):755–767.